Circuits activated by psychiatric-associated behavior: from brain-wide labeling to regional assessment using Psych-TRAP.

Meet Jariwala[1], Xhuliana Sula[1], Emma Kathrine Hjarding[1], Sofie Braum Holst[1], Konstantin Khodosevich[1*]

1. Biotech Research and Innovation Center, BRIC, University of Copenhagen, 2200 Copenhagen, Denmark.

*Corresponding author: Konstantin Khodosevich, konstantin.khodosevich@bric.ku.dk

Abstract

Background: Neuropsychiatric disorders, such as schizophrenia and autism, affect a substantial portion of the global population, 1 in 8 individuals. Genetic risk factors have been the major contribution to neuropsychiatric disorders; however, there is limited knowledge of how risk factors lead to brain circuit impairment and neuropsychiatric phenotypes.

Rationale: Understanding how risk factors impact brain circuitry in the whole brain level at cellular resolution and their connection to neuropsychiatric phenotypes should help develop specific drug targets and therapeutics targeting precisely the affected cell types and circuits.

Methods: We employ a clinically relevant mouse model of one of the major neuropsychiatric genetic risk factors – microdeletion in the 15q13.3 locus. Using the model, we developed a novel technique, Psych-TRAP, to label psychiatric behaviour-associated circuits at whole brain level and at cellular level. We validated the genetic mouse model with clinical phenotypes and labelled transiently active cells, using TRAP2, and quantified cell densities in the whole brain using an automated pipeline, ABBA. This is the first ever approach to validate a triple transgenic mouse line with psychiatric microdeletion and understanding the cellular activation pattern and differential recruitment of cells immediately after a psychiatric-like behavior.

Key findings: Further, we validated Psych-TRAP by understanding the activation of cells in already known brain areas and novel brain areas and confirmed no direct involvement of non-neuronal cells right after 3-chmabered social interaction (3-CSI). Lastly, we discovered the involvement of a dominant GABAergic component in the prefrontal cortex (PFC), mainly mediated by reelin positive (REL+) neurons and by somatostatin positive (SST+) neurons in the primary somatosensory area-trunk (SSp-tr), in mice harbouring 15q13.3 microdeletion.

Future implications: Thus, Psych-TRAP is a robust technique to generate mice line with disrupted copy-number variations, label transiently active cells permanently for future circuit manipulations in an unbiased manner and reveal the underlying molecular markers mediating psychiatric behaviours. This can be extended further to understand the molecular mechanisms of active cells from a particular brain area, identified from Psych-TRAP, using spatial transcriptomics and promises a potential technique for translation research targeting specific manifestations.

Introduction

Our mental health profoundly influences our thoughts, feelings, and behavior. Prioritizing mental well-being is challenging due to individual, societal, genetic and environmental factors and could give rise to psychiatric disorders. Psychiatric disorders comprise a broad group of disorders with a variety of different symptoms. Some of the main classes of psychiatric disorders include neurodevelopmental disorders, depressive disorders, anxiety disorders, eating disorders and psychotic disorders including schizophrenia (1),(2). Common symptoms involve problems with emotional regulation, behavior and cognition (1). Due to overlapping symptoms among different types of disorders, it makes it harder to diagnose and identify drug targets, rendering a high number of misdiagnoses and increasing societal stigma (3). Because of this societal and economic burden, the research field surrounding psychiatric disorders serves a very important role, to an issue that has been growing exponentially the last years. This growing concern makes it crucial to study the cellular correlates of behavior systematically and identify cellular types that governs a specific behavior (4).

The complex nature of the brain makes it harder to understand exactly what contributes to behavioral outcomes. Having a psychiatric phenotype on top of it, adds another layer of complexity to it. Mapping active neural activity after an episode is fundamental in understanding how a given set of cellular assemblies play an active role in mediating behaviours within a specific time-window (5). A combinatorial strategy to label and identify these disrupted circuits and brain areas could explain behavioral deficits related to psychiatry. Currently, most common methods to label activated cellular assemblies with a strong spatial-temporal resolution relies on immediate early genes (IEGs), Ca2+ concentration dependent and release of synaptic vesicles as a measure to indicate activity (6). However, no such technique, to date, is available to label cells in a face-validated genetic model of psychiatry. This is mainly due to complex psychiatric phenotypes and labour-intensive work to make a transactional rodent model (7).

In this study, we propose a novel paradigm (Psych-TRAP) to study psychiatric-like behaviours and label cells, permanently, in the whole brain with high spatial-temporal resolution. A recently developed technique, TRAP2 (8), will capture transiently expressed IEG (FOS), making it possible to label active neurons and circuits permanently. Combining TRAP2 with any face-validated psychiatric mouse model harbouring copy-number variants (CNV) will guide to dissect behavioral symptoms at circuit-level and at cellular-level in a robust model of genetic risk factor associated with psychiatry. We also employed ABBA (9), an automated tool for brain areas registrations and quantification to validate the activation of brain areas. So far, this technique is the first ever attempt to make an intersectional triple transgenic mouse model to study psychiatry and label the activity in the brain in real time, simultaneously.

Results

We propose a combinatorial technique, Psych-TRAP, to tag transiently activated cells after clinically relevant behavior caused due to genetic risk factors, to align with the available mouse brain atlas (10) in a brain-wide manner for automated alignment and annotation. Later, we followed up with region-specific assessment of cells associated with behavioral impairments (**Fig 1A**). The overarching idea of this technique is to generate an intersectional triple transgenic mouse line that reliably recapitulates clinical behavioral symptoms, easy to breed and maintain. To apply our Psych-TRAP technique in a psychiatric risk factor animal model, we crossed the TRAP2; Ai9 reporter mice with mouse model of 15q13.3 microdeletion syndrome (**Fig 1B**). The 15q13.3 locus have been associated with several neuropsychiatric

symptoms in humans. It has gained much attention recently due to its complex genetic architecture, high penetrance, gene-dosage dependent manifestations of phenotypes (11)(12)(13). Previously generated Df(h15q13)/+ mice recapitulate well behavioral and functional changes observed in the patients, specifically in 15q13.3 microdeletion syndrome and in general in neuropsychiatry. Thus, Df(h15q13)/+ mice display psychiatric-like behaviors, including neurophysiological dysfunction, attention deficits, stress responses memory and cell firing impairments, aligning with psychiatric symptoms (14)(15). Below, we refer to this novel intersectional transgenic model as TRAP2-15q$^{+/-}$ (**Fig 1B**).

To visualize the cells activated right after a specific stimulus or behavior, we employed the state-of-the-art knock-in mouse model, TRAP2 (8) on a tdTomato reporter background (TRAP2; Ai9). TRAP2 uses a drug-mediated approach (4-Hydroxy Tamoxifen, 4-OHT) to target inducible CRE (iCre-ER^{T2}) under the FOS promoter, thereby activating the *c-fos*, an immediate early gene, which in-turn activates the floxed tdTomato protein by targeted recombination, exclusively in the active cells (8). Such approach leads to permanent labeling of activated cells. We applied TRAP2-assisted labeling to evaluate a circuit encoding fear memory in the central lateral amygdala (16).

Behavioral signatures of TRAP2-15q$^{+/-}$ recapitulate disrupted social interaction behavior

To deeply understand the behavioral aspects and validate clinically relevant behavioral symptoms in our newly generated mouse line, we subjected the mice carrying TRAP2-15q$^{+/-}$ microdeletion and mice without the microdeletion (wild type (WT) littermates) to a 3-chambered social interaction (3-CSI) paradigm (17). The chamber consists of three zones - social zone (SOC), buffer zone and empty zone (EMP) (**Fig 1C**). SOC harbors a younger mouse of the same gender inside a cage with metal bars to initiate an active social interaction, whereas EMP harbors the empty cage.

After 10 minutes of freely moving behavior, TRAP-WT littermates spent relatively more time in the SOC as compared to EMP, indicating a normal sociability. On the contrary, TRAP2-15q$^{+/-}$ animals showed no such preference in time spent between SOC and EMP (**Fig 1D-E**), indicating a disruptive social interaction behavior. We further zoomed into the sub-divided zones of the 3-CSI, interaction zone (green and yellow color zones around the cage), (**Fig 1C**) and quantified the differences in the time spent by the animal while performing active interaction around the metal cages using a social interaction index (I_{sp}). We observed that TRAP-WT animals significantly spent more time also around the metal cage as opposed to little or negative preference shown by TRAP2-15q$^{+/-}$ mice (**Fig 1F**).

We also quantified how frequent an animal enters the interaction zone in SOC and EMP. We found that TRAP-WT animals made significant number of entries in the SOC, while TRAP2-15q$^{+/-}$ animals showed no preference in the number of entries between SOC and EMP, indicating a lack of motivation to interact actively by TRAP2-15q$^{+/-}$ mice (**Fig 1G**). Lastly, we evaluated movement and velocity of both animal groups and observed no differences (**Fig 1H-I**), confirming that that the lack of social preference is exclusively due to the 15q13.3 microdeletion, and not due to movement impairments. To determine potential sex-specific effects of 15q13.3 microdeletion, we separated females and males for behavioral analyses and found no obvious effects in any behavioral parameters.

As our observations are consistent with the previous studies (18), we have successfully shown that this novel triple transgenic model can be reliably used for our strategy to label and investigate circuitry that is activated by psychiatric-associated behavior.

Whole-brain automated registration and quantification of activated neurons

To identify circuitry that was activated during social interaction behavior (3-CSI) at a brain-wide scale, we aimed to find an accurate and efficient technique for automated brain sections alignment with available an atlas and cell quantification. We injected 4-OHT right after the 3-CSI behavior and left the mice in their respective cages for 7 days to allow targeted recombination in the active cells. We perfuse-fixated the mice and sliced the whole brain coronally. We aligned approximately 17-19 brain sections per mouse from the whole brain with the available Allen Mouse Brain Atlas (10) and quantified using ABBA (9) in an automated manner (**Fig 2A**). These sections were ensured to be corresponding sections from anterior to posterior regions in all animals to maintain the consistency. Representative brain sections (5 sections) are shown in **Fig 2B**, indicating successful alignments of our imaged slices (left) with the mouse brain atlas in anterior to posterior direction (right).

With the help of ABBA (Aligning Big Brains and Atlases), an ImageJ FIJI plugin (9), we quantified the active cells, as observed by tdTomato expression (**Fig 2C**), from all the successfully aligned brain sections. After optimization of successful alignments and filtering out the broken section/regions, we found 474 brain regions to compare the activation pattern of cell densities normalized to the area. The heatmaps in Fig **2D** show top 52 brain regions where we found a systematic difference in the density of activated cells after 3-CSI between TRAP-WT and TRAP2-15q$^{+/-}$ mice.

We observed several cortices and subregions of cortices showing a higher trend of activated cells (**Fig 2D**). The brain region that showed highest differential activation of cells after a psychiatric-like behavior was somatosensory areas, both in primary somatosensory areas (SSp) and supplemental somatosensory areas (SSs) (subregions: SSp-tr5, SSs6a, SSp-bfd6a, SSp-bfd4, SSp-ul, SSp-m6a, SSp-ul6a, SSp-tr4, SSp-m4, SSp-tr, SSp, SSs2/3, SSp-bfd, SSp-n6a, SSp-un4, SSp-n, SSp-bfd2/3). Other cortices that had highest differential activation in TRAP-15q$^{+/-}$ animals as compared to TRAP-WT animals were visual areas (VISam2/3, VISrl4, VISpm5, VISpm, VISrl, VISrl2/3, VISrl1), the whole retrosplenial area (RSP) and sub-regions (RSPagl5, RSPagl2/3), auditory areas (AUDd, AUDd1, AUDd2/3), only one sub-region of gustatory area (GU4), the whole anterior cingulate area (ACA, ACAv, ACAd), posterior agranular insular areas (AIp, AIp5), primary motor area (MOp), posterior parietal association area (PTLp) and olfactory areas such as posterior cortical amygdala areas (COAp, COApm).

In the cortical subplate, we found only anterior basomedial amygdalar area (BMAa) that showed differential activation pattern after 3-CSI in TRAP-15q$^{+/-}$ animals. In the striatal areas, we found higher activation in striatum dorsal region (STRd) which harbors caudate putamen (CP). Among the brainstem areas, we found higher activation of cells in the whole midbrain (MB) overall, where dorsal part of lateral geniculate nucleus (LGd) stands out as the prominent sub-region for higher activation. The only brain region that had highest number of activated cells in TRAP-WT animals was perifornical nucleus (PeF), that is located deep inside the hypothalamus and showed opposite activation pattern than TRAP-15q$^{+/-}$ animals.

ABBA-mediated automated alignment and quantification provided us with an unbiased overview of several brain areas activated after a psychiatric-like behavior. Many of the brain areas from our findings are consistent with several brain areas that were already described in the literature before (19)(20)(21)(22)(23), validating the robustness of this technique. Moreover, we also reported novel brain areas that were not known to play a role in mediating psychiatric phenotypes. Looking deeper into few key regions could reveal the identities of these activated cells and shed some light on their involvement in psychiatric-like behaviors.

Cell-specific labeling among the activated cells in multiple brain regions

We asked what molecular markers these activated cells express. To address this, we focused on key regions of interest that displayed major differences in the number of activated cells (**Fig 2D)**.

We took coronal sections containing primary somatosensory area trunk (SSp-tr), and prefrontal cortex (PFC), harboring anterior cingulate area (ACA), prelimbic area (PL) and infralimbic area (ILA) and compared the densities of activated cells between TRAP-WT and TRAP-15q$^{+/-}$ animals (**Fig 3A, C**). In general, we observed significantly higher number of activated cells in the whole SSp-tr of TRAP-15q$^{+/-}$ mice compared to TRAP-WT mice. Such trend was also preserved along the translaminar structure of SSp-tr, especially in the deeper layers (L5b and L6) (**Fig 3B**). In PFC, the overall quantification also showed significantly higher number of activated cells in TRAP-15+/- mice, especially in ACA and PL (**Fig 3D**).

Then, we aimed to check whether the activation pattern in cells contributing to the psychiatric-like behavior is cell-type specific, owing to differential role of cell types mediating psychiatry (24). We found no involvement of non-neuronal cells that overlap with the activated cells, as stained against widely used molecular markers for microglia (Iba1) and astrocytes (GFAP), in the SSp-tr and the PFC. Instead, almost all the activated cells were found to be neuronal, as validated against the NeuN marker (**Fig 3E-G**).

Recruitment of GABAergic neurons in TRAP2-15q$^{+/-}$ mice after 3-CSI

The inhibitory GABAergic component is involved in etiology of several psychiatric disorders (25)(26)(27), and its imbalance provides the basis of emergence of such disorders (28)(29). We continued further with putative molecular markers of GABAergic neurons (parvalbumin-PV, somatostatin-SST, and reelin-REL) owing to their importance in social behavior and altered states in psychiatry (30)(31)(32)(33)(34).

Firstly, we checked whether there are any differences in the endogenous presence of these putative molecular markers. We quantified the cell densities of PV+, SST+ and Reelin+ cells in SSp-tr and we found no differences in their densities, except for high proportion of PV+ neurons in layer 2-3 (L2-3) in TRAP-WT mice. Although there was a higher trend in the presence of SST+ neurons in TRAP-15q$^{+/-}$, but we did not find any significant differences (**Fig 4A, C, E**). In PFC, we found a striking difference, but only in the density of PV+ neurons where TRAP-WT mice expressed higher PV+ neurons (**Fig 4B, D, F**).

Secondly, we asked whether we observe the activation of GABAergic components after a psychiatric-like behavior in our genetic model. We found a higher proportion of activated GABAergic neurons in the PFC of TRAP2-15q$^{+/-}$ mice, especially in PL, ILA and overall PFC, suggesting an imbalance in the inhibitory/excitatory system where more GABAergic neurons are recruited in the PFC after 3-CSI behavior

(**Fig 5A, B**). Interestingly, we only observed higher trends of activation in SSp-tr of TRAP2-15q$^{+/-}$ mice but there were not significant differences in the overall area as well as its sub-regions (**Fig 5C**).

Lastly, we asked whether we could identify specific GABAergic sub-types among the activated cells and whether we could observe any discrepancy in terms of activation after 3-CSI. We found a selective and consistent pattern of higher proportion of TRAP+ cells co-expressing SST+ marker in SSp-tr in TRAP2-15q$^{+/-}$ mice (**Fig 5D, G-I**), suggesting their crucial role in mediating 3-CSI behavior in a genetic model showing clinical phenotype, but no differential activation pattern in the PFC (**Fig 5J**). We did not find any selective activation pattern in the TRAPed cells expressing PV+ marker, neither in SSp-tr nor PFC among both groups (**Fig 5E, H, K**). We also did not observe differential activation in reelin-positive (REL+) neurons among TRAP+ populations in SSp-tr, except L2-3 in TRAP-15q$^{+/-}$ mice (**Fig 5F, I**). Surprisingly, PFC showed a higher proportion of TRAP+ REL+ neurons in PL, ILA and in the whole PFC of TRAP-15q$^{+/-}$ mice, indicating a crucial role of reelin in mediating psychiatric phenotypes.

Overall, we delineated the differential activation of TRAP+ cells among putative GABAergic sub-types and discovered strong involvement of somatostatin in SSp-tr and reelin in PFC in our genetic model of psychiatry.

Discussion

The Psych-TRAP technique

Here, we have proposed Psych-TRAP technique where we used the combinatorial techniques, for the first time, to label transiently active neurons (using TRAP2) (8) in a genetic model of psychiatry (Df(h15q13)/+) (15) displaying clinical phenotypes, and later performing automated alignment and quantification to understand the activation pattern in the whole brain using ABBA (9). We have successfully demonstrated and validated a reliable model and behavior to perform exploration and confirmatory studies. This can be extended to discover new brain areas and looking deeper to reveal the molecular identities of the activated cells. Psych-TRAP technique addresses a major problem in cell quantification strategy in a brain-wide manner. Conventional cell counting in the whole brain is time consuming and tedious and hence only few sections were used to quantify, rendering several important sections uncounted (35). Also, we address this need to use whole brain quantification strategy in a face-validated genetic model of psychiatry, which has never been demonstrated before in this combination.

Semi-automated quantification has been optimized by several techniques like SHARCQ (36), FASTMAP (37), AMaSiNe (38), however, they also come with limitations of requiring coding and anatomy skills, disproportionate alignment and not ability to quantify cells in automated manner. In contrast, ABBA (9) offers an automated pipeline to align brain sections automatically using Allen Brain Atlas CCF (10) in an open-source ImageJ Fiji software and integrating the automated quantification into another open-source QuPath software.

Previous studies used psychiatric models to understand the brain connectivity and activation using f-MRI and BOLD imaging (39)(40)(41), but it requires expensive instruments and expertise to perform such analyses. Psych-TRAP provides an unbiased approach to employ any genetic model of psychiatry along with existing TRAP2 technique (8) without compromising on clinical phenotypes and later use it for discovering novel brain areas using ABBA (9) without any expertise on coding or anatomy.

In this study, Psych-TRAP proved to be efficient in overcoming all those problems and the novel triple transgenic mouse model (**Fig 1A-B**) did not compromise on psychiatric-like phenotypes (**Fig 1E-I**). Later, Psych-TRAP revealed previously known and novel brain areas that are differentially activated after 3-CSI, indicating a robustness of its future applications (**Fig 2**). So, in all aspects Psych-TRAP proved to be the most efficient technique that integrates a genetic component, labels temporally active cells and performs automated counting in the whole brain.

Impact of 15q13.3 microdeletion on mouse social behavior

TRAP-WT mice displayed a clear preference towards the stranger mouse (**Fig 1**), a finding consistent with previous studies (42)(43)(18). This observation aligns with the established understanding that mice are generally considered a social species, justifying the need for social interaction in their environment needs (44). Contrary to TRAP-WT mice, TRAP-15q$^{+/-}$ mice displayed a lack of preference of social interactions and in the number of entries in the social zone, also in consistent with finding that has been previously reported (18).

Furthermore, we reported that TRAP-15q$^{+/-}$ mice displayed impairments in their social preference index further substantiating their social deficits. A notable remark pertaining to the social preference index is the great disparity between the behavioral responses of TRAP-WT and TRAP-15q$^{+/-}$ mice. While TRAP-WT mice consistently demonstrated positive values indicative of a pronounced social preference, TRAP-15q$^{+/-}$ mice exhibited a spectrum of responses, spanning from markedly negative to strongly positive values in their indices. Such responses may potentially be associated with the phenotypic behavioral variability characterizing human carriers (45). Furthermore, the high variability in the penetrance of the microdeletion observed in humans (46), could contribute to the heterogeneity of social behaviors in the mouse model (18).

In addition to assessing parameters related to the social behavior of mice, we evaluated their velocities and movement patterns, and we observed no differences in locomotion, proving that the impaired social behavior is exclusively due to the genetic 15q13.3 micro-deletion. Also, it was reported before that Df(h15q13)/+ mice did not display exploratory tendencies, locomotory abilities during open field task (18). We also compared gender-specific alterations in their social preferences and we found that the effect of 15q13.3 microdeletion consistently affected both sexes and their impaired social behavior is conserved across groups (**Fig 1**).

Behavior-induced neuronal activation in a brain-wide manner using ABBA alignment

After validating the behavioral impairments in our novel triple transgenic model, we employed Psych-TRAP for whole brain automated alignment and quantification of cells activated after 3-CSI. This was possible due to injection of 4-OHT right after the behavior that enables targeted recombination in active cells, where newly formed FOS was labelled with a time window of 2-4 hours of peak expression (8). This prevents non-specific site-specific recombination in non-active cells, providing a decent temporal resolution. We reported successful alignments and counting from 474 brain regions and found 52 brain areas with differential cell densities (**Fig 2**).

We observed the activation mostly in cortical areas. Several regions are consistent with the activation patterns described in the literature (19)(20)(21)(22)(23)(47). Somatosensory areas (primary somatosensory area (SSp) and supplemental somatosensory area (SSs)) were among the highest brain areas that displayed higher activation in cell densities after 3-CSI in TRAP2-15q$^{+/-}$ mice. Somatosensory areas play a key role in sensory processing and experience-dependent behavioral adaptations (48)(22). The differences were not only limited to the overall area of SS, but also to their subregions (SSp-tr5, SSs6a, SSp-bfd6a, SSp-bfd4, SSp-ul, SSp-m6a, SSp-ul6a, SSp-tr4, SSp-m4, SSp-tr, SSs2/3, SSp-bfd, SSp-n6a, SSp-un4, SSp-n, SSp-bfd2/3). Such differences are expected to arise as there are several studies indicating layer-specific roles in sensory-motor integration (49)(50).

Another key region that is strongly associated with social behavior and psychiatric phenotypes in anterior cingulate area (ACA) which has been validated consistently to play major roles in shaping social information (30)(51) and serves as an information transfer region between limbic system and cognitive system (52). There has been no direct links for involvement of visual areas (VISam2/3, VISrl4, VISpm5, VISpm, VISrl, VISrl2/3, VISrl1) in social interaction, but there is a study indicating the correlation of *TRPM1* gene, present on the 15q13.3 locus, with visual abnormalities (53). A study recently highlighted the importance of visual areas during social behavior and can influence decisions (54).

The higher activation in RSP is evident due to its anatomical connectivity and receives synaptic inputs from visual areas, hippocampus and thalamic nuclei and consequently playing a role in various roles like social behavior, processing sensory information, spatial information processing in psychiatric models of mice (55)(56)**.** The role of primary motor areas (MOp) is to perform fine-motor controls and co-ordinates inputs from and to other brain regions (57)(58). The role of insular cortex is well established in social exploration and social behavior (59)(60), however we demonstrated for the first time the role of posterior agranular insular area (AIp, AIp5) linked to a psychiatric-like phenotype.

It is surprising to observe higher activation in MOp in TRAP2-15q$^{+/-}$ mice in our study, even though the movement and velocity across both groups remains unchanged (**Fig 1**). This indicates future possibilities to investigate complex motor behaviors in our model. Another novel brain area that we observed and was not directly linked to social behavior or psychiatry is gustatory area (GU4), which plays role in taste encoding and decision making (61).

Differential activation of neuronal sub-types after a psychiatric-like behavior

We zoomed into SSp-tr and PFC to dig deeper into revealing the subtypes of activated cells. We saw no involvement of non-neuronal cells like microglia (Iba1+) and astrocytes (GFAP+) among the TRAP+ cells after 3-CSI (**Fig 3**). It could be because their expression in the cells may not be directly correlated to their roles, but microglia-derived or associated factors like neuregulin and BDNF could contribute as an indirect way to influence social interaction behavior (62)(63). The activation of cortical astrocytes also works in the similar fashion, as they are not directly recruited during 3-CSI but downstream calcium signaling pathways can modulate social interaction deficits in autism models (64)(65). Also, there are reports of loss of astrocytes in Df(h15q13)/+ mouse model (66), but in our study, we did not see any differences in activation of TRAP+ GFAP+ cells in SSp-tr and PFC in both groups, indicating there is no direct involvement post 3-CSI or the activation of GFAP+ neurons follow different dynamics and hence not captured.

The 15q13.3 microdeletion has pleiotropic effects on individuals and causes varied phenotypes. The effect of the microdeletion starts affecting from as early as prenatal brain development and makes changes in the transcriptome pattern (67). The excitation/inhibition balance has been known to be compromised in various psychiatric disorders caused by copy number variations in different brain areas (68)(28)(26)(14). We expected to see higher activation of GABAergic neurons in our regions of interest, as somatosensory areas receive several first order sensory inputs and thalamic inputs (69). However, we did not observe such imbalance in the activation of GABAergic neurons in SSp-tr after 3-CSI (**Fig 5**). There are evidence that exhibition/inhibition ratio (E/I ratio) is increased in psychiatric models in somatosensory areas (70) and that could be the reason that GABAergic component is not dominating after 3-CSI. The E/I ratio in PFC have been widely discussed in psychiatric disorders and social interaction (26)(71)(72) but their role in 15q13.3 microdeletion right after a psychiatric-like episode is less studied. We observed a strong activation of GABAergic component in the PFC after 3-CSI (**Fig 5**). Such discrepant findings in SSp-tr and PFC indicate complex circuitry control in these brain areas arising due to the 15q13.3 microdeletion. Further analysis in other brain areas could answer this discrepancy and address the imbalance in E/I ratio better.

The role of PV+, SST+ and Rel+ neurons have been implicated in social behaviors (30)(32)(73)(74)(75)(76)(77), but their roles in 15q13.3 microdeletion mouse model after a psychiatric-like behavior has not been studied before. Using Psych-TRAP, we revealed the strong involvement of SST+ neurons in SSp-tr and REL+ in PFC regions of the brain. Surprisingly, PV+ neurons do not show to play an immediate role after 3-CSI in either of the brain areas.

Future implications

Psych-TRAP enables users to label stimulus-specific populations in combination with genetic mouse models of psychiatry harboring copy-number variations (CNVs). There are various CNVs which have potential to undergo functional studies (78) and were never used to study due to factors like unreliable phenotypes and failure of discovery of novel therapeutic targets (79). In this study, we overcame this problem by using 15q13.3 microdeletion mouse model to capture cell populations after 3-CSI. The 15q13.3 microdeletion mouse model was used, until now, for face validating clinical phenotypes and electrophysiological studies and was not used to understand at the cellular resolution (14)(15)(18)(80). These populations are labeled with a strong-temporal resolution in a permanent fashion and can be manipulated for functional studies in future, such as optogenetics and chemogenetics. To achieve spatial resolution, a user can also take help of Cre-Lox mediated viral vectors in TRAP2 mice (not crossed with Ai9 reporter mice) where fluorescent labeling of active cells is dependent on which brain area a vector is transfected (81).

Thus, Psych-TRAP is a valuable and handy technique to address clinical symptoms, discovering novel brain areas and molecular targets underlying complex psychiatric phenotypes. Combining Psych-TRAP with spatial transcriptomics, however tedious, can open ways for transcriptomic profiling of active populations.

Limitations

Psych-TRAP uses TRAP2 labelling approach and captures newly formed FOS protein, making it harder to capture populations that express other immediate early genes (IEGs) like *Arc* and *Npas4* (82). It can be limiting to behaviours orchestrated by other IEGs. Furthermore, the concentration of the delivered 4-OHT, that binds to the iCRE and causes recombination, is important since it defines the total amount of labeled neurons. However, a minimum threshold of 4-OHT concentration needs to be achieved to observe any positive signal, but not too high to cause unspecific labeling in the brain areas. We have optimized the concentration of 4-OHT in this study to 30 mg/kg to attain a detectable threshold. Another limitation of this study is the relatively lower number of females harboring 15q13.3 microdeletion and therefore it is hard to decipher any major conclusions for gender-specific behavior alterations. It would be interesting to study the genetic penetrance of this CNV across genders and generations. ABBA alignment also offers some limitations as it is hard to align and quantify sections that are broken, distorted or missing. Automated counting marks it as 'zero' cells, if a brain area is not found.

Overall, Psych-TRAP has strong potential to revolutionize modern labeling strategies and functional studies that take psychiatric models into account.

Figure 1

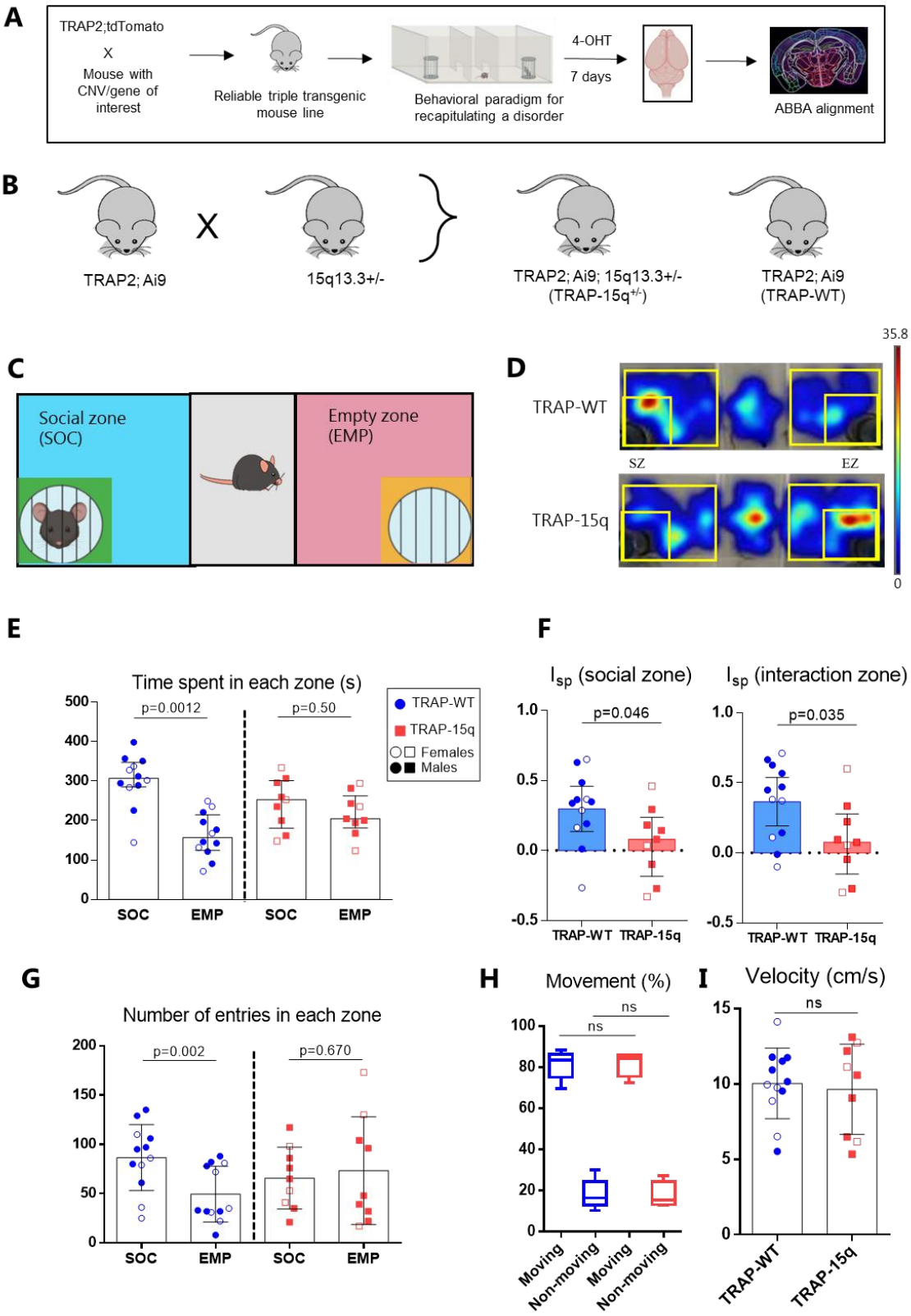
A
TRAP2;tdTomato
X
Mouse with CNV/gene of interest
Reliable triple transgenic mouse line
Behavioral paradigm for recapitulating a disorder
4-OHT
7 days
ABBA alignment
B
TRAP2; Ai9
X
15q13.3+/-
TRAP2; Ai9; 15q13.3+/-
(TRAP-15q+/-)
TRAP2; Ai9
(TRAP-WT)
C
Social zone
(SOC)
Empty zone
(EMP)
D
TRAP-WT
TRAP-15q
SZ
EZ
35.8
0
E
Time spent in each zone (s)
p=0.0012
p=0.50
TRAP-WT
TRAP-15q
Females
Males
SOC
EMP
SOC
EMP
F
Isp (social zone)
Isp (interaction zone)
p=0.046
p=0.035
TRAP-WT
TRAP-15q
TRAP-WT
TRAP-15q
G
Number of entries in each zone
p=0.002
p=0.670
SOC
EMP
SOC
EMP
H
Movement (%)
ns
ns
Moving
Non-moving
Moving
Non-moving
I
Velocity (cm/s)
ns
TRAP-WT
TRAP-15q

Figure 1: The Psych-TRAP technique.

A: Proposal of a novel Psych-TRAP technique and timeline to make an intersectional transgenic mouse line, label active cells, align brain sections and quantify in an automated manner.

B: Generation of a triple transgenic mouse line, yielding TRAP-15q$^{+/-}$ and TRAP-WT mice.

C: 3-chambered social interaction test apparatus (3-CSI). Blue and pink chambers are social (SOC) zones and empty zones (EMP). Green and yellow zones are their respective interaction zones.

D: Heatmaps of two representative animals form TRAP-WT and TRAP-15q$^{+/-}$ groups showing the amount of time spent in the apparatus. Color bar represents red as high intensity and blue as low intensity.

E: Time spent by animals in each zone in seconds (s). Blue filled dots are TRAP-WT mice and red filled squares are TRAP-15q$^{+/-}$ mice. Male mice are denoted by black filled circle and square and female mice are denoted by clear circle and square. SOC: social zone, EMP: empty zone. (TRAP-WT: n=12 mice, SOC: 302.1±19.08, EMP: 162.6±16.16, paired t-test p=0.0012; TRAP-15q$^{+/-}$: n=9 animals, SOC: 243.8±21.43, EMP: 216.4±18.00, paired t-test p=0.50).

F: Social preference index (I_{sp}) of social zone (TRAP-WT: n=12 mice, 0.297±0.074; TRAP-15q$^{+/-}$: n=9 mice, 0.055±0.085, unpaired t-test with Welch's correction p=0.046) and interaction zone (TRAP-WT: n=12 mice, 0.365±0.08; TRAP-15q$^{+/-}$: n=9 mice, 0.088±0.092, unpaired t-test with Welch's correction p=0.035).

G: Number of entries in each zone (TRAP-WT: n=12, SOC 86.58±9.68, EMP 49.50±8.15, Wilcoxon test p=0.002; TRAP-15q$^{+/-}$: n=9, SOC 65.78±10.48, EMP 73.44±18.23, paired t test p=0.670).

H: Movement (%). Blue represents TRAP-WT mice and red represents TRAP-15q$^{+/-}$.

I: Velocity (cm/s). Blue represents TRAP-WT mice and red represents TRAP-15q$^{+/-}$.

All data are represented as ± S.E.M, $p<0.05$.

Figure 2

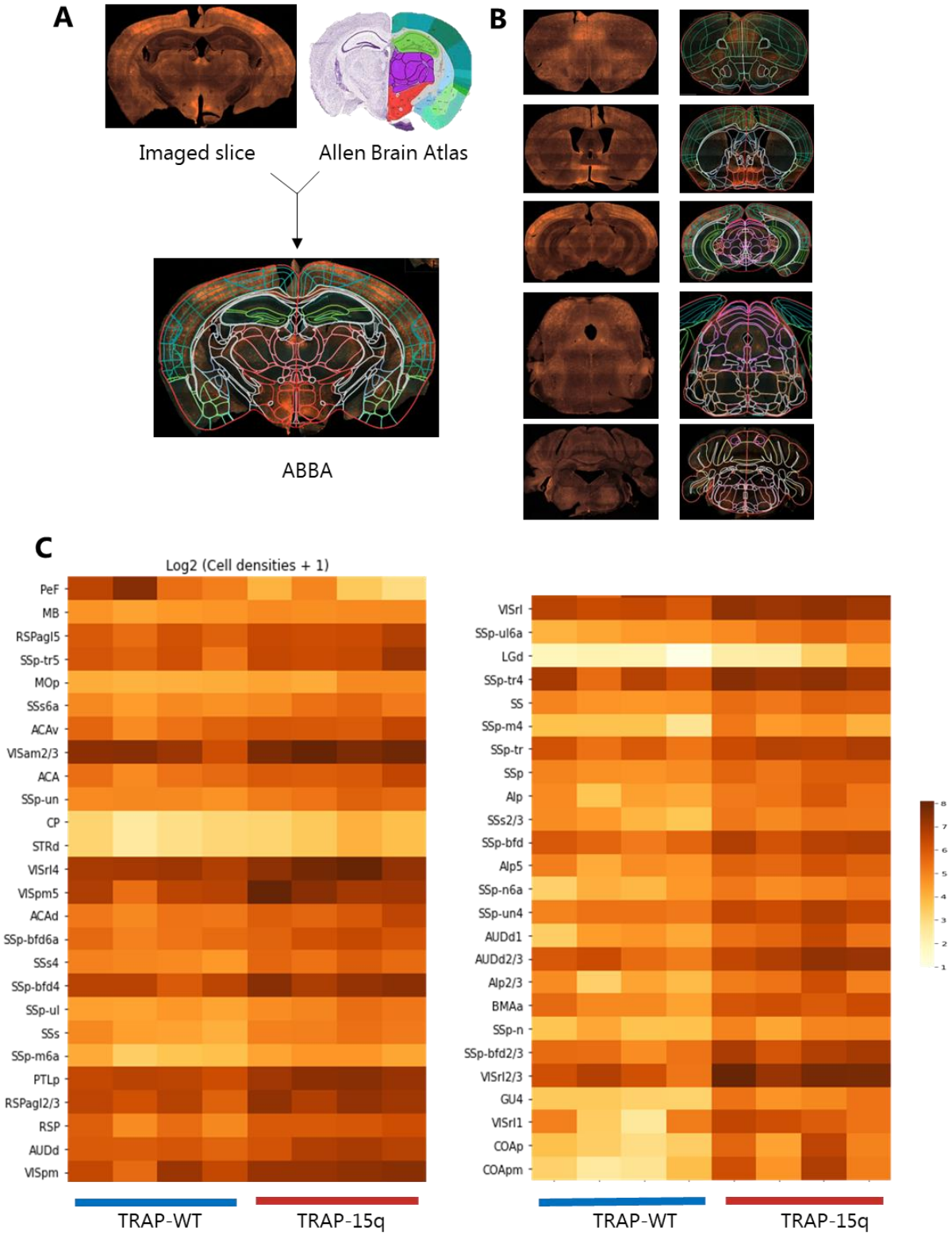
A
Imaged slice
Allen Brain Atlas
ABBA
B
C
Log2 (Cell densities + 1)
PeF
MB
RSPagl5
SSp-tr5
MOp
SSs6a
ACAv
VISam2/3
ACA
SSp-un
CP
STRd
VISrl4
VISpm5
ACAd
SSp-bfd6a
SSs4
SSp-bfd4
SSp-ul
SSs
SSp-m6a
PTLp
RSPagl2/3
RSP
AUDd
VISpm
TRAP-WT
TRAP-15q
VISrl
SSp-ul6a
LGd
SSp-tr4
SS
SSp-m4
SSp-tr
SSp
Alp
SSs2/3
SSp-bfd
Alp5
SSp-n6a
SSp-un4
AUDd1
AUDd2/3
Alp2/3
BMAa
SSp-n
SSp-bfd2/3
VISrl2/3
GU4
VISrl1
COAp
COApm
TRAP-WT
TRAP-15q
8
7
6
5
4
3
2
1

Figure 2: Automated alignment, registration and quantification using ABBA.

A: Strategy to combine imaged slice (left) and corresponding slice from Allen Brain Atlas CCF (right), yielding an example of a successful alignment (below).

B: Representative examples from 5 brain slices, anterior to posterior, proving successful alignments using ABBA.

C: Heatmaps of log2(cel densities +1) showing 52 brain areas from TRAP-WT and TRAP-15q$^{+/-}$ mice (4 mice per group, blueline below indicates TRAP-WT and red line below indicates TRAP-15q$^{+/-}$) that showed a differential activation of cells.

Figure 3

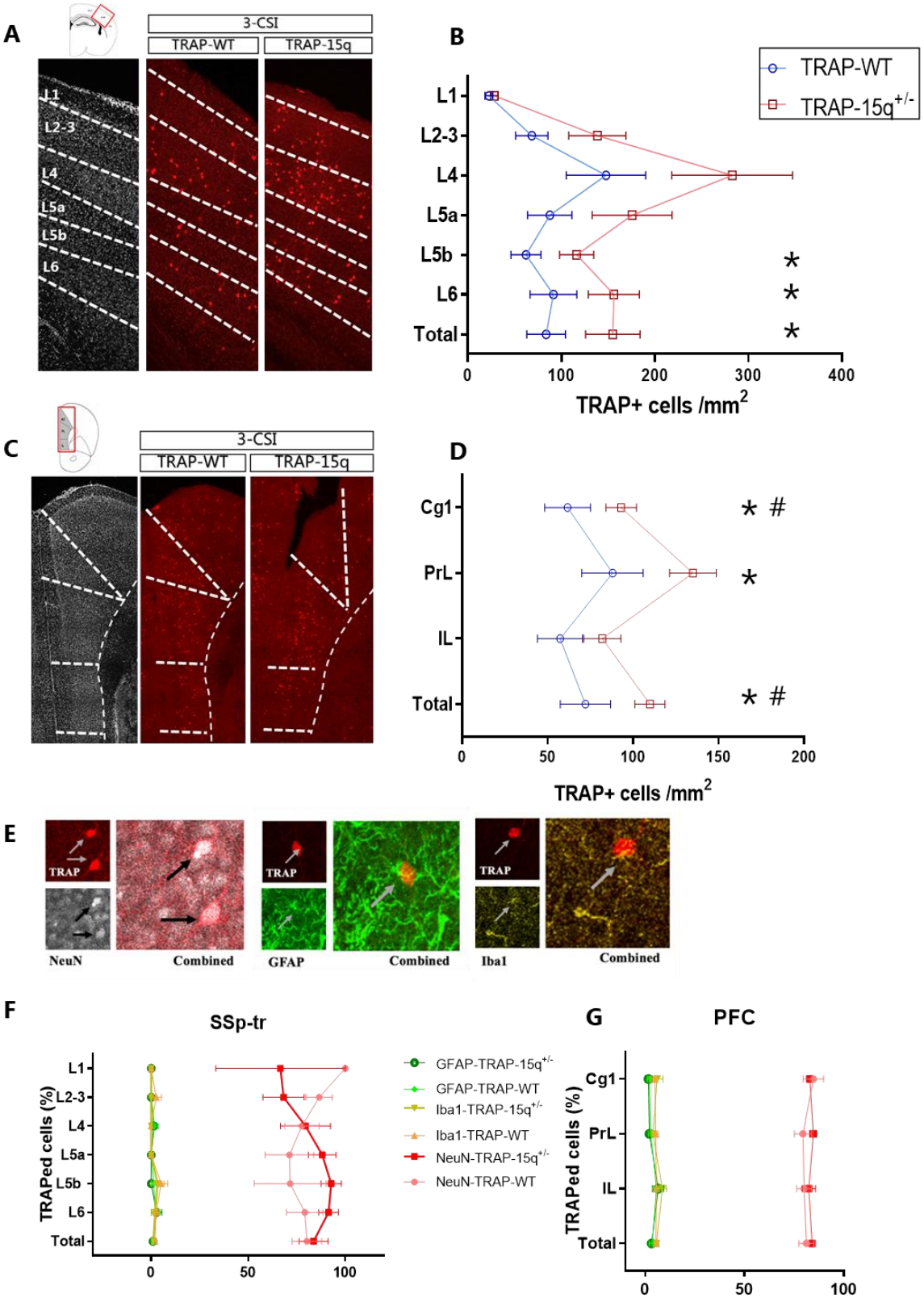
A
3-CSI
TRAP-WT
TRAP-15q
L1
L2-3
L4
L5a
L5b
L6
B
TRAP-WT
TRAP-15q+/-
L1
L2-3
L4
L5a
L5b
L6
Total
*
*
*
0
100
200
300
400
TRAP+ cells /mm2
C
3-CSI
TRAP-WT
TRAP-15q
D
Cg1
PrL
IL
Total
* #
*
* #
0
50
100
150
200
TRAP+ cells /mm2
E
TRAP
NeuN
Combined
TRAP
GFAP
Combined
TRAP
Iba1
Combined
F
SSp-tr
TRAPed cells (%)
L1
L2-3
L4
L5a
L5b
L6
Total
0
50
100
GFAP-TRAP-15q+/-
GFAP-TRAP-WT
Iba1-TRAP-15q+/-
Iba1-TRAP-WT
NeuN-TRAP-15q+/-
NeuN-TRAP-WT
G
PFC
TRAPed cells (%)
Cg1
PrL
IL
Total
0
50
100

Figure 3: Differential patterns of activated cells in SSp-tr and PFC.

A: Representative sections of SSp-tr from TRAP-WT and TRAP-15q$^{+/-}$ mouse, after 3-CSI and successful labeling. Index represents an outline of the brain area where the magnified area is highlighted in red box. First section in grays is DAPI staining to identify layers in SSp-tr. Red fluorescent cells are tdTomato+ cells that are labeled after 3-CSI.

B: Quantification of cell densities in sub-regions of SSp-tr between TRAP-WT (n=10) (blue) and TRAP-15q$^{+/-}$ (n=9) (red) mice.

C: Representative sections of PFC from TRAP-WT and TRAP-15q$^{+/-}$ mouse, after 3-CSI and successful labeling. Index represents an outline of the brain area where the magnified area is highlighted in red box. First section in grays is DAPI staining to identify layers in PFC.

D: Quantification of cell densities in sub-regions of PFC between TRAP-WT (n=10) (blue) and TRAP-15q$^{+/-}$ (n=9) (red) mice.

E: Representative sections of immunostaining against a neuronal marker (NeuN), astrocyte marker (GFAP) and a microglia marker (Iba1) along with TRAP+ cells expressing tdTomato.

F: Quantification of TRAP+ cells co-expressing NeuN (TRAP-WT n=6, TRAP-15q$^{+/-}$ n=4), Iba1 (TRAP-WT n=5, TRAP-15q$^{+/-}$ n=3) and GFAP (TRAP-WT n=3, TRAP-15q$^{+/-}$ n=3) in SSp-tr in percentages.

G: Quantification of TRAP+ cells co-expressing NeuN (TRAP-WT n=6, TRAP-15q$^{+/-}$ n=4), Iba1 (TRAP-WT n=5, TRAP-15q$^{+/-}$ n=3) and GFAP (TRAP-WT n=3, TRAP-15q$^{+/-}$ n=3) in PFC in percentages.

Figure 4

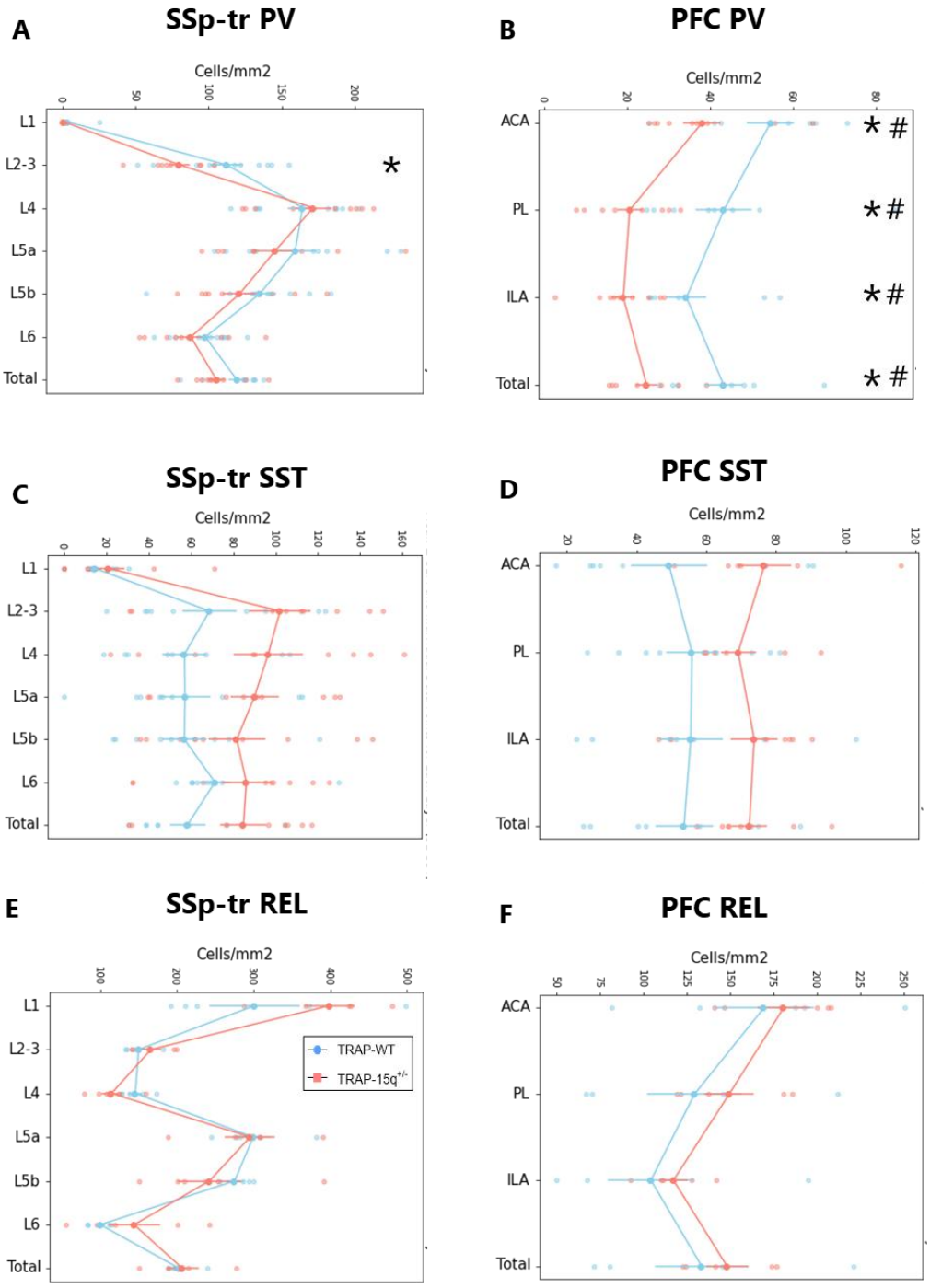
A
SSp-tr PV
Cells/mm2
L1
L2-3
L4
L5a
L5b
L6
Total
*
B
PFC PV
Cells/mm2
ACA
PL
ILA
Total
* #
* #
* #
* #
C
SSp-tr SST
Cells/mm2
D
PFC SST
Cells/mm2
E
SSp-tr REL
Cells/mm2
TRAP-WT
TRAP-15q+/-
F
PFC REL
Cells/mm2

Figure 4: Quantification of endogenous putative GABAergic markers in SSp-tr and PFC across subregions.

A-B: Quantification of parvalbumin (PV) positive neurons. (TRAP-WT n=10, TRAP-15q$^{+/-}$ n=9).

C-D: Quantification of somatostatin (SST) positive neurons. (TRAP-WT n=9, TRAP-15q$^{+/-}$ n=9).

E-F: Quantification of reelin (REL) positive neurons. (TRAP-WT n=5, TRAP-15q$^{+/-}$ n=5).

Figure 5

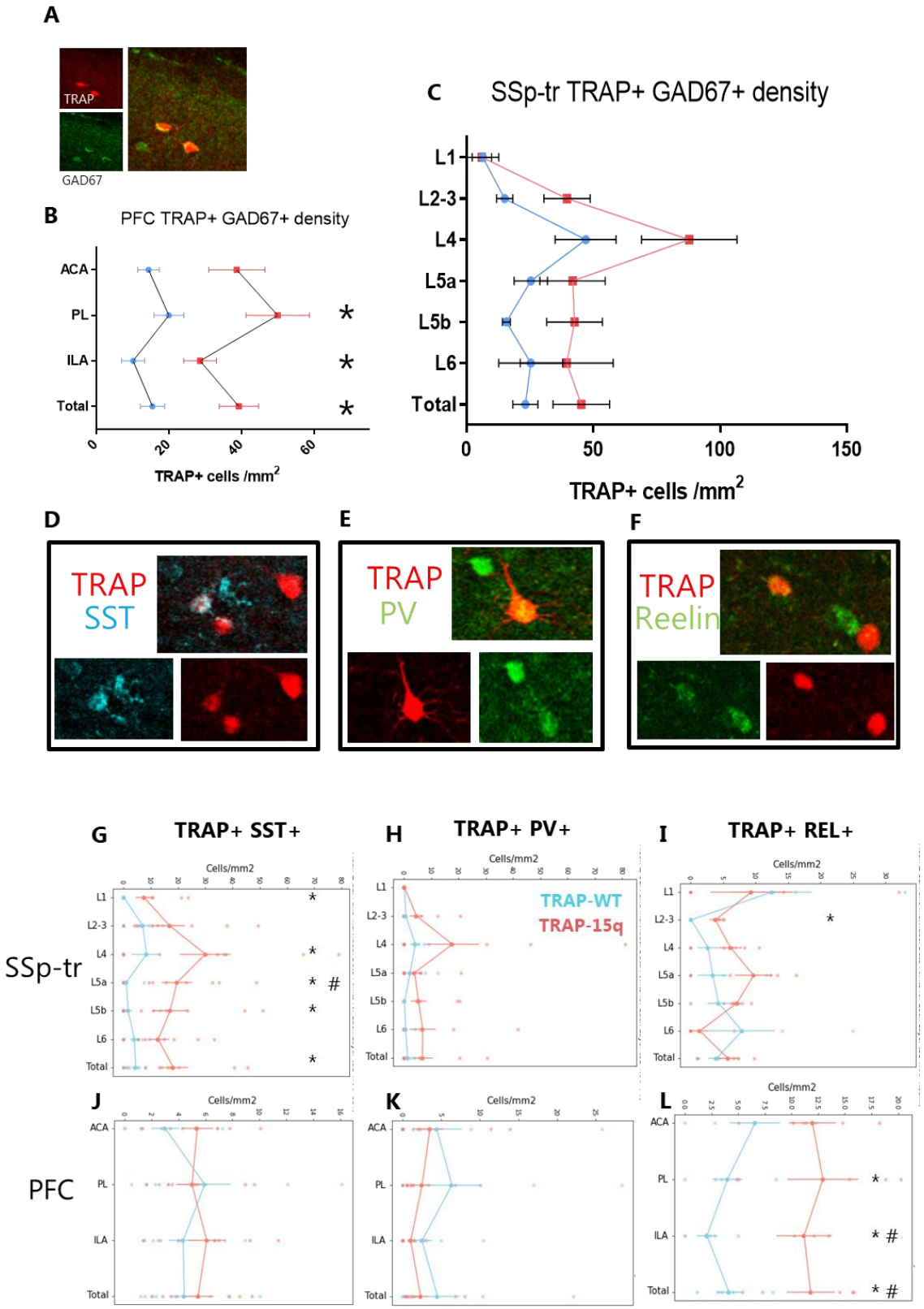
A
TRAP
GAD67
B
PFC TRAP+ GAD67+ density
ACA
PL
ILA
Total
0
20
40
60
TRAP+ cells /mm2
C
SSp-tr TRAP+ GAD67+ density
L1
L2-3
L4
L5a
L5b
L6
Total
0
50
100
150
TRAP+ cells /mm2
D
TRAP
SST
E
TRAP
PV
F
TRAP
Reelin
G
TRAP+ SST+
H
TRAP+ PV+
I
TRAP+ REL+
Cells/mm2
TRAP-WT
TRAP-15q
SSp-tr
J
K
L
PFC

Figure 5: Recruitment of GABAergic neurons in TRAP2-15q+/- mice after 3-CSI.

A: Representative image of immunostaining against GAD67 marker with TRAP+ cells in SSp-tr.

B: Quantification of TRAP+ cell densities co-expressing GAD67+ in PFC. (TRAP-WT n=4, TRAP-15q$^{+/-}$ n=5).

C: Quantification of TRAP+ cell densities co-expressing GAD67+ in SSp-tr. (TRAP-WT n=4, TRAP-15q$^{+/-}$ n=5).

D-F: Representative images of immunostaining against somatostatin (SST), parvalbumin (PV) and reelin (REL) markers.

G-I: Quantifications of TRAP+ cell densities co-expressing SST (TRAP-WT n=9, TRAP-15q$^{+/-}$ n=9), PV (TRAP-WT n=10, TRAP-15q$^{+/-}$ n=9) and REL (TRAP-WT n=5, TRAP-15q$^{+/-}$ n=5) in SSp-tr.

J-L: Quantifications of TRAP+ cell densities co-expressing SST (TRAP-WT n=8, TRAP-15q$^{+/-}$ n=7), PV (TRAP-WT n=8, TRAP-15q$^{+/-}$ n=9) and REL (TRAP-WT n=5, TRAP-15q$^{+/-}$ n=5) in PFC.

Methods

Animal husbandry

The TRAP2-WT mice were generated by crossing TRAP2 mice (Jackson Laboratory: 030323) with Ai9 reporter mice (Jackson Laboratory 007909). Furthermore, to create the triple transgenic animal line, the TRAP2-WT mice were crossed with (Df(15q13)/+) mice (Taconic Biosciences 10962) yielding TRAP-15q$^{+/-}$ mice. All three genes were kept in heterozygous manner and animals containing homozygous genotypes were not included in the study. The wildtype (TRAP-WT) animals in this project were TRAP2; Ai9 mice that did not contain the 15q13.3 microdeletion. The mice were housed together in IVS cages. The mice had ad-libitum access to food and water along with sawdust and other nesting materials present in all cages. The conditions (temperature regulation, ventilation and humidity) were constantly controlled, and the mice were following a reversed 12-hour cycle. Mice were single-housed for 4 days prior to the experiment for habituation and were kept in the same cage for 7 days after 4-Hydroxy tamoxifen (4-OHT) injection. The cages were discarded following the animal laboratory guidelines. The mice used for the experiment were older than 60 days, which is equivalent to minimum 20 years in humans (83). The ethical guidelines of the National Animal Ethic Committee of Denmark and Danish legislation were followed during all animal handling and experimenting.

Genotyping

To determine whether the mice had the genetic combinations needed for the experiment, genotyping of each animal was carried out. The primers used for detection were as follows:

TRAP2 wild forward: GTC CGG TTC CTT CTA TGC AG (357 bp)

TRAP2 common: GAA CCT TCG AGG GAA GAC G (heterozygote 357 bp + 232 bp)

TRAP2 mutant forward: CCT TGC AAA AGT ATT ACA TCA CG (232 bp)

tdTomato (Ai9) wild type pair (AAG GGA GCT GCA GTG GAG TA and CCG AAA ATC TGT GGG AAG TC)

tdTomato (Ai9) mutant pair (GGC ATT AAA GCA GCG TAT CC and CTG TTC CTG TAC GGC ATG G)

Df(15q13)/+ wild type pair (CTGTATCCGTAAACACGCTAACTGG and GAGCAGTGTTTGTGTGGTTTATGG)

Df(15q13)/+ mutant pair (TCGAGCCTAGGCATAACTTCGTATA and TCGGCACCTTGATGAGTCTTG)

13,5 µL of each primer MIX was added to PCR tubes. Extracted DNA from animal's ear clip was added to the prospective PCR wells. Pictures of the electrophoresis gel were captured and the genotype for each test animal were determined.

As shown in this figure, genotyping results indicate #176 as TRAP-WT (heterozygous bands for Fos and tdTomato, but wild type band for 15q) and #209 as TRAP-15q$^{+/-}$ (heterozygous bands for all). Animals with other genotyping combinations were either used for subsequent breeding or control experiments.

Preparation of 4-OHT

Labelling of active neurons during behavior was done by injection of 4-OHT intra peritoneally right after the behavior. This was done to label freshly formed FOS proteins produced along with endogenous FOS proteins. The 4-OHT solution was prepared fresh before the experiment and was protected from light. This was done to avoid evaporation and stability of 4-OHT. 4-OHT comes in powder form and dissolves only in organic solvent like Di-methyl sulfoxide (DMSO). 4-OHT-DMSO solution can be stored at -20 for months. The solution for the experiment was prepared by thawing 4-OHT-DMSO solution, mixed with Tween80 (2%) and diluted with saline (9mg/ml). Animals were injected according to weight with 30 mg/kg of an adult mouse. The injection was done intraperitoneally. After animals were injected with the 4-OHT solution, they were housed separately in disposable cages for 7 days undisturbed. Because of the harmfulness of 4-OHT, being carcinogenic in nature, all procedures were carried out while wearing adequate protective equipment and everything was discarded in yellow boxes according to animal authority guidelines given by the Department of Experimental Medicine, Copenhagen University.

Habituation

Before the experiments were conducted, habituation of mice was carried out to avoid unnecessary stress to the animal and animal getting acquainted with the experimenter. This was done by single housing the test mice for four days before the behavior experiments, to ensure a strong want for social interaction and lifting and pinching the mice on lower abdomen to mimic the action of injection of 4-OHT on the test day. This was done to make sure that the injection caused the least amount of stress to the test animal which would affect the activation and thereby TRAP labelling of neurons. Stranger mice were also habituated for 4-7 days for 10 minutes prior to the test day to sit calmly inside the metal cage.

Behavior

A 3-chamber social interaction (3-CSI test) was used to assess the mice's social interaction. The behavior was assessed in all mice. The 3-CSI test setup is shown in **Fig 1C**. The stranger mouse was always chosen as the younger mouse of the same gender as the mouse being analysed. To begin with, the test mouse was placed in the buffer zone, and the behavior of the mouse was then tracked for 10 minutes. Between every behavior, the apparatus was cleaned using 70% ethanol, to avoid olfactory overstimulation of the new test animal due to smells from the previous stranger mouse and test mouse.

Behavior analysis

During the behavior, the experimental mice were placed in the buffer zone and allowed to freely explore the arena for 10 min. Their behavior was recorded with a ceiling-mounted camera and later it was tracked and scored by the EthoVision XT software (Noldus). The software was trained to track the nose point of the test mice. The automated tracking was followed by manual review of the footage by the experimenter, to ensure that software derived tracking mistakes are corrected. Active interaction was considered when the mouse directly interacts with the metal wired-cage, directly faces towards it and sniffs around the

wired-cage. Non-interaction was considered when the mouse was in the vicinity of the wired cage but facing another way and self-grooming in the proximity of the cage. The experimenter is blinded to the genotype during the behavior scoring.

Perfuse-fixation

Before perfusion, the animals were anesthetized using Ketamine (100mg/ml)-Xylazine (20mg/ml) cocktail. When the animals were unresponsive to pain stimuli, the animals were cut open to access the heart. Then the animals were perfused by flushing the blood out using PBS and then flushing with 4% Paraformaldehyde (PFA) to fixate the brain tissue. After fixation, the brains were collected and were put in PFA overnight. Next day, the brains were transferred to PBS where it was then stored.

Vibratome slicing and mounting

The collected brains were sliced using the Leica VT1000s vibratome. The brains were sliced in coronal slices of 100 µm. To prevent decomposition and fungal growth the slices were stored in a mixture of PBS containing 0,02% sodium azide and were kept at 4°C. Approximately 16-19 slices per brain, with 600 µm between the slices, were picked anterior to posterior (AP: +3.0 mm to -5.0 mm) to get an overview of the whole brain. The chosen slices were then washed in PBS 2x for 5 minutes. Afterwards, the slices were stained with DAPI (1:50000) for 10 minutes. After the DAPI staining, slices were washed again in PBS 3x for 2 minutes. The stained slices were then carefully, using a paint brush, mounted on Superfrost microscope slides, and were cover slipped using FluromountG medium. After mounting, the slides were stored in a 4°C fridge in a closed container to protect it from light.

Imaging

Imaging was done using Zeiss confocal microscope LSM800. The 10x magnification objective was used and images were captured for all slices. The z-axis was set to get the maximum intensity of the tdTomato and was made sure that all parts of the brain slice were visible. Consistent parameters were maintained across all images.

ABBA alignment and quantification

The pipeline was followed as mentioned in the original article (9). Cell detection parameters were optimized to get consistent positive cells across the slice and across all animals.

Statistical analysis

Images were generated in GraphPad Prism 6 and Python. All data were tested for normality using Shapiro-Wilk normality test. Appropriate posthoc tests were carried out for paired and unpaired data. Heatmaps for whole brain quantification were generated by normalizing the raw cell counts per slice with area of the brain region. All sections were pulled into single file and brain areas that were missing out in at least one animal (due to fracture, breakage during slicing or taking brain out of the mice or folding of slices), were excluded to have an unbiased approach of most differential brain areas. Normalized cell densities were transformed into log2 (x+1), where x is cell density of each brain area. Medians of each group were compared by Mann-Whitney U test. For heatmap analysis, we did not perform FDR due to low number of mice per group.

References

1. Cao H, Wang J, Baranova A, Zhang F. Classifying major mental disorders genetically. Prog Neuropsychopharmacol Biol Psychiatry. 2022;112:110410.

2. Uher R, Zwicker A. Etiology in psychiatry: embracing the reality of poly-gene-environmental causation of mental illness. World psychiatry. 2017;16(2):121–9.

3. Wainberg ML, Scorza P, Shultz JM, Helpman L, Mootz JJ, Johnson KA, et al. Challenges and opportunities in global mental health: a research-to-practice perspective. Curr Psychiatry Rep. 2017;19(5):28.

4. Scangos KW, State MW, Miller AH, Baker JT, Williams LM. New and emerging approaches to treat psychiatric disorders. Nat Med. 2023;29(2):317–33.

5. Kaiser T, Feng G. Modeling psychiatric disorders for developing effective treatments. Nat Med. 2015;21(9):979–88.

6. Nagahama K, Jung VH, Kwon HB. Cutting-edge methodologies for tagging and tracing active neuronal coding in the brain. Curr Opin Neurobiol. 2025;92:102997.

7. Nestler EJ, Hyman SE. Animal models of neuropsychiatric disorders. Nat Neurosci. 2010;13(10):1161–9.

8. Allen WE, DeNardo LA, Chen MZ, Liu CD, Loh KM, Fenno LE, et al. Thirst-associated preoptic neurons encode an aversive motivational drive. Science (1979). 2017;357(6356):1149–55.

9. Chiaruttini N, Castoldi C, Requie LM, Camarena-Delgado C, Dal Bianco B, Gräff J, et al. ABBA+ BraiAn, an integrated suite for whole-brain mapping, reveals brain-wide differences in immediate-early genes induction upon learning. Cell Rep. 2025;44(7).

10. Wang Q, Ding SL, Li Y, Royall J, Feng D, Lesnar P, et al. The Allen mouse brain common coordinate framework: a 3D reference atlas. Cell. 2020;181(4):936–53.

11. Chamberlain SJ. RNAs of the human chromosome 15q11-q13 imprinted region. Wiley Interdiscip Rev RNA. 2013;4(2):155–66.

12. Van Bon BWM, Mefford HC, Menten B, Koolen DA, Sharp AJ, Nillesen WM, et al. Further delineation of the 15q13 microdeletion and duplication syndromes: a clinical spectrum varying from non-pathogenic to a severe outcome. J Med Genet. 2009;46(8):511–23.

13. Williams NM, Franke B, Mick E, Anney RJL, Freitag CM, Gill M, et al. Genome-wide analysis of copy number variants in attention deficit hyperactivity disorder: the role of rare variants and duplications at 15q13. 3. American Journal of Psychiatry. 2012;169(2):195–204.

14. Nilsson SRO, Celada P, Fejgin K, Thelin J, Nielsen J, Santana N, et al. A mouse model of the 15q13. 3 microdeletion syndrome shows prefrontal neurophysiological dysfunctions and attentional impairment. Psychopharmacology (Berl). 2016;233(11):2151–63.

15. Fejgin K, Nielsen J, Birknow MR, Bastlund JF, Nielsen V, Lauridsen JB, et al. A mouse model that recapitulates cardinal features of the 15q13. 3 microdeletion syndrome including schizophrenia-and epilepsy-related alterations. Biol Psychiatry. 2014;76(2):128–37.

16. Hou WH, Jariwala M, Wang KY, Seewald A, Lin YL, Liou YC, et al. Inhibitory fear memory engram in the mouse central lateral amygdala. Cell Rep. 2024;43(8).

17. Rein B, Ma K, Yan Z. A standardized social preference protocol for measuring social deficits in mouse models of autism. Nat Protoc. 2020;15(10):3464–77.

18. Kogan JH, Gross AK, Featherstone RE, Shin R, Chen Q, Heusner CL, et al. Mouse model of chromosome 15q13. 3 microdeletion syndrome demonstrates features related to autism spectrum disorder. Journal of Neuroscience. 2015;35(49):16282–94.

19. Li H, Zhao Z, Jiang S, Wu H. Brain circuits that regulate social behavior. Mol Psychiatry. 2025;1–17.

20. Xu S, Jiang M, Liu X, Sun Y, Yang L, Yang Q, et al. Neural circuits for social interactions: from microcircuits to input-output circuits. Front Neural Circuits. 2021;15:768294.

21. Guo B, Chen J, Chen Q, Ren K, Feng D, Mao H, et al. Anterior cingulate cortex dysfunction underlies social deficits in Shank3 mutant mice. Nat Neurosci. 2019;22(8):1223–34.

22. Kim Y, Venkataraju KU, Pradhan K, Mende C, Taranda J, Turaga SC, et al. Mapping social behavior-induced brain activation at cellular resolution in the mouse. Cell Rep. 2015;10(2):292–305.

23. Perkins AE, Woodruff ER, Chun LE, Spencer RL, Varlinskaya E, Deak T. Analysis of c-Fos induction in response to social interaction in male and female Fisher 344 rats. Brain Res. 2017;1672:113–21.

24. Brennand KJ, Simone A, Tran N, Gage FH. Modeling psychiatric disorders at the cellular and network levels. Mol Psychiatry. 2012;17(12):1239–53.

25. Chattopadhyaya B, Cristo G Di. GABAergic circuit dysfunctions in neurodevelopmental disorders. Front Psychiatry. 2012;3:51.

26. Malwade S, Gasthaus J, Bellardita C, Andelic M, Moric B, Korshunova I, et al. Identification of vulnerable interneuron subtypes in 15q13. 3 microdeletion syndrome using single-cell transcriptomics. Biol Psychiatry. 2022;91(8):727–39.

27. Xu M yi, Wong AHC. GABAergic inhibitory neurons as therapeutic targets for cognitive impairment in schizophrenia. Acta Pharmacol Sin. 2018;39(5):733–53.

28. Sylvester AL, Hensenne E, Ivanov D, Poser BA, Linden DEJ, van Amelsvoort T, et al. Neural excitation/inhibition imbalance and neurodevelopmental pathology in human copy number variant syndromes: a systematic review. J Neurodev Disord. 2025;17(1):31.

29. Batiuk MY, Tyler T, Dragicevic K, Mei S, Rydbirk R, Petukhov V, et al. Upper cortical layer–driven network impairment in schizophrenia. Sci Adv. 2022;8(41):eabn8367.

30. Qi C, Sima W, Mao H, Hu E, Ge J, Deng M, et al. Anterior cingulate cortex parvalbumin and somatostatin interneurons shape social behavior in male mice. Nat Commun. 2025;16(1):4156.

31. Jindal K, Ringland A, Fitzcharles S, Redd C, Wheeler DG, Coutellier L. Npas4 drives the effects of early social isolation on social behaviors and prefrontal parvalbumin neurons. Prog Neurobiol. 2025;102810.

32. Sánchez-Hidalgo AC, Martín-Cuevas C, Crespo-Facorro B, Garrido-Torres N. Reelin alterations, behavioral phenotypes, and brain anomalies in schizophrenia: a systematic review of insights from rodent models. Front Neuroanat. 2022;16:844737.

33. Dienel SJ, Wade KL, Fish KN, Lewis DA. Alterations in Prefrontal Cortical Somatostatin Neurons in Schizophrenia: Evidence for Weaker Inhibition of Pyramidal Neuron Dendrites. Biol Psychiatry. 2025;

34. Liu L, Xu H, Wang J, Li J, Tian Y, Zheng J, et al. Cell type–differential modulation of prefrontal cortical GABAergic interneurons on low gamma rhythm and social interaction. Sci Adv. 2020;6(30):eaay4073.

35. Courtney JM, Morris GP, Cleary EM, Howells DW, Sutherland BA. Automated quantification of multiple cell types in fluorescently labeled whole mouse brain sections using QuPath. Bio Protoc. 2022;12(13):e4459–e4459.

36. Lauridsen K, Ly A, Prévost ED, McNulty C, McGovern DJ, Tay JW, et al. A semi-automated workflow for brain slice histology alignment, registration, and cell quantification (SHARCQ). eNeuro. 2022;9(2).

37. Terstege DJ, Oboh DO, Epp JR. FASTMAP: open-source flexible atlas segmentation tool for multi-area processing of biological images. eNeuro. 2022;9(2).

38. Song JH, Choi W, Song YH, Kim JH, Jeong D, Lee SH, et al. Precise mapping of single neurons by calibrated 3D reconstruction of brain slices reveals topographic projection in mouse visual cortex. Cell Rep. 2020;31(8).

39. Choe KY, Bethlehem RAI, Safrin M, Dong H, Salman E, Li Y, et al. Oxytocin normalizes altered circuit connectivity for social rescue of the Cntnap2 knockout mouse. Neuron. 2022;110(5):795–808.

40. Zerbi V, Pagani M, Markicevic M, Matteoli M, Pozzi D, Fagiolini M, et al. Brain mapping across 16 autism mouse models reveals a spectrum of functional connectivity subtypes. Mol Psychiatry. 2021;26(12):7610–20.

41. Bertero A, Liska A, Pagani M, Parolisi R, Masferrer ME, Gritti M, et al. Autism-associated 16p11. 2 microdeletion impairs prefrontal functional connectivity in mouse and human. Brain. 2018;141(7):2055–65.

42. Kaidanovich-Beilin O, Lipina T, Vukobradovic I, Roder J, Woodgett JR. Assessment of social interaction behaviors. J Vis Exp. 2011;(48):2473.

43. Nadler JJ, Moy SS, Dold G, Trang D, Simmons N, Perez A, et al. Automated apparatus for quantitation of social approach behaviors in mice. Genes Brain Behav. 2004;3(5):303–14.

44. Zhu P, Liu W, Zhang X, Li M, Liu G, Yu Y, et al. Correlated evolution of social organization and lifespan in mammals. Nat Commun. 2023;14(1):372.

45. Ziats MN, Grosvenor LP, Rennert OM. Functional genomics of human brain development and implications for autism spectrum disorders. Transl Psychiatry. 2015;5(10):e665–e665.

46. Ben-Shachar S, Chahrour M, Thaller C, Shaw CA, Zoghbi HY. Mouse models of MeCP2 disorders share gene expression changes in the cerebellum and hypothalamus. Hum Mol Genet. 2009;18(13):2431–42.

47. Kim H, Ährlund-Richter S, Wang X, Deisseroth K, Carlén M. Prefrontal parvalbumin neurons in control of attention. Cell. 2016;164(1):208–18.

48. Waiblinger C, McDonnell ME, Reedy AR, Borden PY, Stanley GB. Emerging experience-dependent dynamics in primary somatosensory cortex reflect behavioral adaptation. Nat Commun. 2022;13(1):534.

49. Ayaz A, Stäuble A, Hamada M, Wulf MA, Saleem AB, Helmchen F. Layer-specific integration of locomotion and sensory information in mouse barrel cortex. Nat Commun. 2019;10(1):2585.

50. Senzai Y, Fernandez-Ruiz A, Buzsáki G. Layer-specific physiological features and interlaminar interactions in the primary visual cortex of the mouse. Neuron. 2019;101(3):500–13.

51. Kitagawa K, Takemoto T, Seiriki K, Kasai A, Hashimoto H, Nakazawa T. Socially activated neurons in the anterior cingulate cortex are essential for social behavior in mice. Biochem Biophys Res Commun. 2024;726:150251.

52. Stevens FL, Hurley RA, Taber KH. Anterior cingulate cortex: unique role in cognition and emotion. J Neuropsychiatry Clin Neurosci. 2011;23(2):121–5.

53. Hori T, Ikuta S, Hattori S, Takao K, Miyakawa T, Koike C. Mice with mutations in Trpm1, a gene in the locus of 15q13. 3 microdeletion syndrome, display pronounced hyperactivity and decreased anxiety-like behavior. Mol Brain. 2021;14(1):61.

54. Greer D, Lei T, Kryshtal A, Jessen ZF, Schwartz GW. Visual identification of conspecifics shapes social behavior in mice. Current Biology. 2025;35(2):287–99.

55. Shi Y, Yan J, Xu X, Qiu Z. Gating of social behavior by inhibitory inputs from hippocampal CA1 to retrosplenial agranular cortex. Neurosci Bull. 2024;40(11):1635–48.

56. Shang HF, Cai R, Sun H, Sheng T, Lian YN, Liu L, et al. Deconstruction of the retrosplenial granular cortex for social behavior in the mouse model of fragile X syndrome. bioRxiv. 2021;2021.

57. Lee C, Kim Y, Kaang BK. The primary motor cortex: the hub of motor learning in rodents. Neuroscience. 2022;485:163–70.

58. Carmona LM, Nelson A, Tun LT, Kim A, Shiao R, Kissner MD, et al. Corticothalamic neurons in motor cortex have a permissive role in motor execution. Nat Commun. 2025;16(1):4735.

59. Miura I, Sato M, Overton ETN, Kunori N, Nakai J, Kawamata T, et al. Encoding of social exploration by neural ensembles in the insular cortex. PLoS Biol. 2020;18(9):e3000584.

60. Glangetas C, Guillaumin A, Ladevèze E, Braine A, Gauthier M, Bonamy L, et al. A population of Insula neurons encodes for social preference only after acute social isolation in mice. Nat Commun. 2024;15(1):7142.

61. Lin JY, Katz DB. Gustatory cortex: Taste coding and decision making in one. Current biology. 2024;34(11):R542–3.

62. Ikawa D, Makinodan M, Iwata K, Ohgidani M, Kato TA, Yamashita Y, et al. Microglia-derived neuregulin expression in psychiatric disorders. Brain Behav Immun. 2017;61:375–85.

63. Komori T, Okamura K, Ikehara M, Yamamuro K, Endo N, Okumura K, et al. Brain-derived neurotrophic factor from microglia regulates neuronal development in the medial prefrontal cortex and its associated social behavior. Mol Psychiatry. 2024;29(5):1338–49.

64. Wang Q, Kong Y, Wu DY, Liu JH, Jie W, You QL, et al. Impaired calcium signaling in astrocytes modulates autism spectrum disorder-like behaviors in mice. Nat Commun. 2021;12(1):3321.

65. Allen M, Huang BS, Notaras MJ, Lodhi A, Barrio-Alonso E, Lituma PJ, et al. Astrocytes derived from ASD individuals alter behavior and destabilize neuronal activity through aberrant Ca2+ signaling. Mol Psychiatry. 2022;27(5):2470–84.

66. Al-Absi AR, Qvist P, Glerup S, Sanchez C, Nyengaard JR. Df (h15q13)/+ mouse model reveals loss of astrocytes and synaptic-related changes of the excitatory and inhibitory circuits in the medial prefrontal cortex. Cerebral Cortex. 2021;31(3):1609–21.

67. Körner MB, Velluva A, Bundalian L, Radtke M, Lin CC, Zacher P, et al. Altered gene expression profiles impair the nervous system development in individuals with 15q13. 3 microdeletion. Sci Rep. 2022;12(1):13507.

68. Sohal VS, Rubenstein JLR. Excitation-inhibition balance as a framework for investigating mechanisms in neuropsychiatric disorders. Mol Psychiatry. 2019;24(9):1248–57.

69. Sato M, Nakai N, Fujima S, Choe KY, Takumi T. Social circuits and their dysfunction in autism spectrum disorder. Mol Psychiatry. 2023;28(8):3194–206.

70. Gibson JR, Bartley AF, Hays SA, Huber KM. Imbalance of neocortical excitation and inhibition and altered UP states reflect network hyperexcitability in the mouse model of fragile X syndrome. J Neurophysiol. 2008;100(5):2615–26.

71. Funk M, Schuelert N, Jaeger S, Dorner-Ciossek C, Rosenbrock H, Mack V. Activation of group II metabotropic receptors attenuates cortical EI imbalance in a 15q13. 3 microdeletion mouse model. bioRxiv. 2020;2020–9.

72. Gao R, Peterson EJ, Voytek B. Inferring synaptic excitation/inhibition balance from field potentials. Neuroimage. 2017;158:70–8.

73. Jeon YS, Jeong D, Kweon H, Kim JH, Kim CY, Oh Y, et al. Adolescent parvalbumin expression in the left orbitofrontal cortex shapes sociability in female mice. Journal of Neuroscience. 2023;43(9):1555–71.

74. Li X, Sun H, Zhu Y, Wang F, Wang X, Han L, et al. Dysregulation of prefrontal parvalbumin interneurons leads to adult aggression induced by social isolation stress during adolescence. Front Mol Neurosci. 2022;15:1010152.

75. Smith CJ, Kingsbury MA, Dziabis JE, Hanamsagar R, Malacon KE, Tran JN, et al. Neonatal immune challenge induces female-specific changes in social behavior and somatostatin cell number. Brain Behav Immun. 2020;90:332–45.

76. Wang X, Chen M, Mei D, Shi S, Guo J, Gao C, et al. Somatostatin-expressing interneurons of prefrontal cortex modulate social deficits in the Magel2 mouse model of autism. Mol Autism. 2025;16(1):18.

77. Sivasangari K, Rajan KE. Prenatal exposure to valproic acid alters Reelin, NGF expressing neuron architecture and impairs social interaction in their autistic-like phenotype male offspring. Exp Brain Res. 2022;240(7):2005–16.

78. Mollon J, Schultz LM, Huguet G, Knowles EEM, Mathias SR, Rodrigue A, et al. Impact of copy number variants and polygenic risk scores on psychopathology in the UK Biobank. Biol Psychiatry. 2023;94(7):591–600.

79. Uliana DL, Zhu X, Gomes F V, Grace AA. Using animal models for the studies of schizophrenia and depression: The value of translational models for treatment and prevention. Front Behav Neurosci. 2022;16:935320.

80. Forsingdal A, Fejgin K, Nielsen V, Werge T, Nielsen J. 15q13. 3 homozygous knockout mouse model display epilepsy-, autism-and schizophrenia-related phenotypes. Transl Psychiatry. 2016;6(7):e860–e860.

81. Lesuis SL, Rashid AJ, Hoorn A, Park S, Mocle AJ, Torelli AM, et al. Protocol to visualize three distinct neuronal ensembles encoding different events in the mouse brain using genetic and viral approaches. STAR Protoc. 2025;6(2):103747.

82. Franceschini A, Costantini I, Pavone FS, Silvestri L. Dissecting neuronal activation on a brain-wide scale with immediate early genes. Front Neurosci. 2020;14:569517.

83. Khodosevich K, Sellgren CM. Neurodevelopmental disorders—high-resolution rethinking of disease modeling. Mol Psychiatry. 2023;28(1):34–43.